ISBN: 978-3-95450-236-3 ISSN: 2673-7027 doi:10.18429/JACoW-eeFACT2022-THXAS0102

STATUS AND EXPERIENCES OF THE VACUUM SYSTEM IN THE SuperKEKB MAIN RING

T. Ishibashi[1,2 †], Y. Suetsugu[1,2], K. Shibata[1,2], M. Shirai[1], S. Terui[1], K. Kanazawa[1,2], H. Hisamatsu[1], M. L. Yao[2]
[1]KEK Accelerator Laboratory, Tsukuba, Ibaraki, Japan
[2]SOKENDAI, Hayama, Kanagawa, Japan

Abstract

Since the SuperKEKB began operation in 2016, the stored beam currents in the main ring have been gradually increased. When the system was commissioned in the Spring of 2022, the maximum beam currents were ~1460 mA in the low-energy ring for positrons (LER) and ~1145 mA in the high-energy ring for electrons (HER). The beam doses are ~7312 Ah in the LER and ~6199 Ah in the HER, and vacuum scrubbing of the beam pipes is proceeding well. However, during these operations, problems such as abnormal pressure rises, vacuum leaks, and collimator damage have occurred. Here, we report on our experiences and the status of the vacuum system after its commissioning in the spring of 2019, known as Phase 3.

INTRODUCTION

The SuperKEKB accelerator is an electron–positron collider with storage rings [1]. The main ring consists of a low-energy ring (LER) for positrons (beam energy: 4 GeV; designed beam current: 3.6 A) and high-energy ring (HER) for electrons (beam energy: 7 GeV; designed beam current: 2.6 A), both with a circumference of about 3 km. Cessation of the operation of the KEKB accelerator ceased in 2010 was followed by about six years of construction of upgrades. During this period, approximately 93% of the vacuum components in the LER and approximately 20% of those in the HER were newly developed and installed [2]. Fig. 1 show the layout of the SuperKEKB main ring. Names of vertical and horizontal collimators are indicated by the letters V and H, respectively. The ring has four arc sections and four straight sections. IR: interaction region; SC: superconducting cavity region; ARES: normal-conducting RF cavity region. The ring is divided in to 12 sections, D01 to D12. Figure 2 shows a photograph of an arc-section of the ring, where: IP is ion pump; NEG is nonevaporable getter pump. Rectifiers are installed in the heater of the NEG pumps and in bending magnets in the LER, and are used to activate these while the magnets are excited

The SuperKEKB main ring began operating in 2016, and this first commissioning stage from February to June of that year was named Phase 1 [3, 4]. The second commissioning stage from March to July of 2018 was named Phase 2, and a positron-damping ring (DR) was introduced after this stage [5, 6]. In 2019, a full-scale physics experiment with the Belle II detector started; this was named Phase 3, which continues to the present.

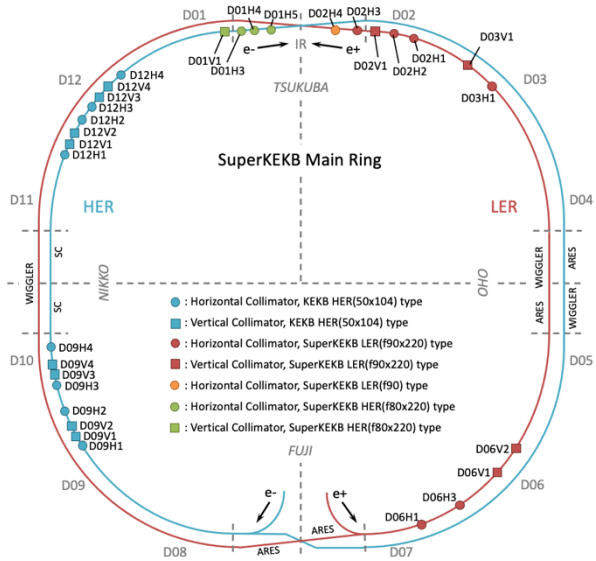

Figure 1: Layout of the SuperKEKB main ring.

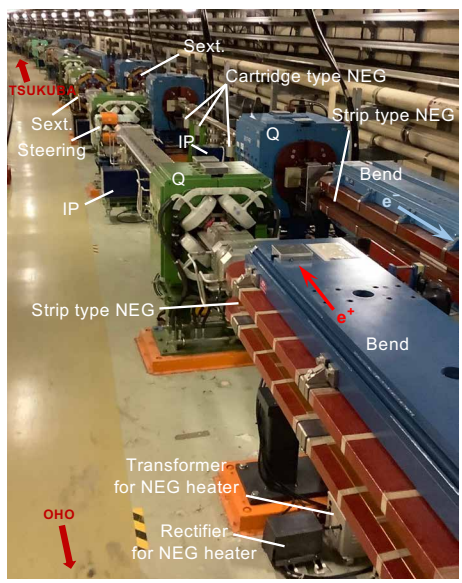

Figure 2: Photograph of an arc-section of the SuperKEKB main ring.

After breaking the world record for luminosity in 2020 [7], SuperKEKB has continued to set new records. The record peak luminosity was ~4.7×10^{34} cm^{-2} s^{-1} with 1.4 A in the LER and 1.1 A in the HER when the stored bunch number was 2249 during the spring run of 2022 [8].

† takuya.ishibashi@kek.jp

Content from this work may be used under the terms of the CC-BY-4.0 licence (© 2022). Any distribution of this work must maintain attribution to the author(s), title of the work, publisher, and DOI

ISBN: 978-3-95450-236-3 ISSN: 2673-7027 doi:10.18429/JACoW-eeFACT2022-THXAS0102

The highest stored beam current is ~1460 mA for the LER and ~1145 mA for the HER. The vacuum components newly developed and introduced for SuperKEKB generally operate as expected. However, troubles, such as vacuum leaks, sometimes occur, most of which are caused by the thermal load from the synchrotron radiation (SR).

The upgrading of the vacuum system and the status of the vacuum system from the start of operation in 2016 to Phase 2 operation in 2018 have been previously reported [3–6, 9, 10]. Here, we report mainly on our experiences and the current status of the SuperKEKB vacuum system since Phase 3 operation began in 2019.

OPERATION STATUS

In upgrading from KEKB to SuperKEKB, various vacuum components were newly developed and introduced. As a countermeasure to electron-cloud instability in the LER, titanium nitride (TiN)-coated beam pipes were installed almost all the way around the ring, together with beam pipes with antechambers, beam pipes with a groove structure, a clearing electrode, and permanent magnets to induce a magnetic field in the longitudinal direction [11, 12]. In addition, as a countermeasure to impedance, gate valves and bellows chambers equipped with comb-type radio-frequency (RF) shields [13], newly developed collimators [14], MO flanges with very small steps in the vacuum seal part were adopted, among other equipment [2]. These components have generally been working as expected since the start of the operation.

Figure 3 shows the operation time for each of the last six years, the percentage of time when problems were encountered, and the percentage of vacuum system that suffered problems.

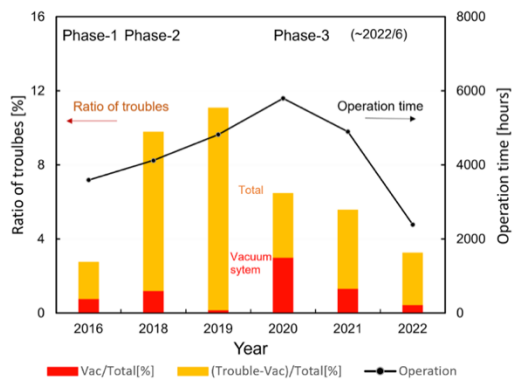

Figure 3: Operating time, ratios of total machine problems, and vacuum-system-related problems for each year since 2016.

The problems referred to here are those that stopped the beam operation. The percentage of the problems related to the vacuum systems was ~4% or less. The main vacuum-system-related problems are air leaks at flanges. In addition, collimators, especially those in the vertical direction, were frequently damaged by beam hits. In 2020 and 2021, the fact that the damaged collimator was replaced during the operating period is also a factor that increased the problem time related to the system.

Vacuum Scrubbing

The pressure increase Δp [Pa] per unit beam current ΔI [A] as a function of the beam dose in the LER and HER from the start of SuperKEKB operation to the end of the latest commissioning period on June 2022 is shown in Fig. 4. The figure also shows the photon-stimulated-desorption (PSD) coefficient η [molecules photon^{-1}] for the photon dose. The beam dose and photon dose [15] are calculated by using the following expressions:

$$(\text{beam dose}) = \int_{t_0}^{t_1} I(t)\,dt \qquad (1)$$

$$(\text{photon dose}) = 8.08 \times 10^{11} \frac{E}{L} \int_{t_0}^{t_1} I(t)\,dt, \qquad (2)$$

where I is the beam current I [A], E is the beam energy [eV], L is the photon-irradiated length [m], t_0 and t_1 are the start time of the SuperKEKB operation and the end time of the latest commissioning period. L, the total approximate length of the arc-sections in the rings, is assumed to be 2000 m.

Sets consisting of an ion pump and a cold-cathode ionization gauge (CCG) are installed around each ring at intervals of approximately 10 m. The pressure given is the average of the values indicated by the CCGs (these are conversion values in the case of nitrogen). However, the pressure at the beam channel where the beam actually passes was estimated by simulation to be approximately three times higher than that at the position where the CCGs are installed so in this paper we use a value three times the value indicated by the CCG for the pressure. The lower limit of the pressure measurement by the CCGs is 1×10^{-8} Pa. Then, in the calculations for Fig. 4, the pressure increase is divided by the beam current when the beam current is 40% or more of the maximum value at a given time.

PSD coefficient is calculated using a following formula:

$$\eta = \frac{S_{\text{eff}}}{8.08 \times 10^{11} kTE} \frac{\Delta p}{\Delta I}, \qquad (3)$$

where S_{eff} is the effective pumping speed [m^{3}s^{-1}], k is the Boltzmann constant [J K^{-1}], and T is the temperature [K]. In calculating η, we assumed pumping speeds of 0.06 and 0.03 m^{3}s^{-1}m^{-1} in the LER and HER, respectively, and T = 300 K.

As of June 2022, the LER achieved $\Delta p/\Delta I < 1 \times 10^{-7}$ Pa A^{-1} for the whole ring and $\eta < 5 \times 10^{-7}$ molecules photon^{-1} at the arc sections with a beam dose of ~7312.1 A h. Then, the HER achieved $\Delta p/\Delta I < 1 \times 10^{-8}$ Pa A^{-1} for the whole ring and $\eta < 2 \times 10^{-8}$ molecules photon^{-1} or less at the arc sections with a beam dose of ~6199.0 A h. The value of $\Delta p/\Delta I$ in the HER is smaller than that in the LER because most of the beam pipes have been reused since the KEKB era, and their surfaces have been scrubbed for longer times than those of newly installed beam pipes.

Content from this work may be used under the terms of the CC-BY-4.0 licence (© 2022). Any distribution of this work must maintain attribution to the author(s), title of the work, publisher, and DOI

ISBN: 978-3-95450-236-3 ISSN: 2673-7027 doi:10.18429/JACoW-eeFACT2022-THXAS0102

Content from this work may be used under the terms of the CC-BY-4.0 licence (© 2022). Any distribution of this work must maintain attribution to the author(s), title of the work, publisher, and DOI

For LER, another beam dose of ~43400 A h is required for $\Delta p/\Delta I$ to reach 1×10^{-8} Pa A^{-1}, which is approximately the same as the present level in the HER by extrapolation using the results of a regression analysis. The achieved beam dose in the LER during the 2022 spring run was ~440 A h month^{-1}, so it would take about 99 months operation to achieve 10^{-8} Pa A^{-1} if we assume the achieved dose rate in the latest commissioning period. In fact, the stored beam current is intended to gradually increase during future operations, so this could be achieved in a shorter operating time. Then, as the beam current increased, a pressure increase due to heating was observed especially in the LER, but note that this effect is not taken into consideration in the present discussion.

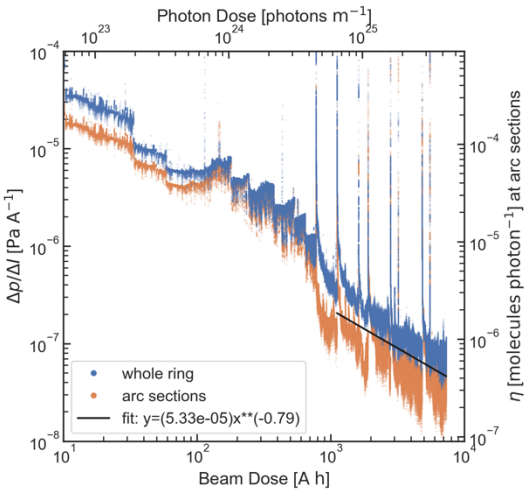

(a) LER

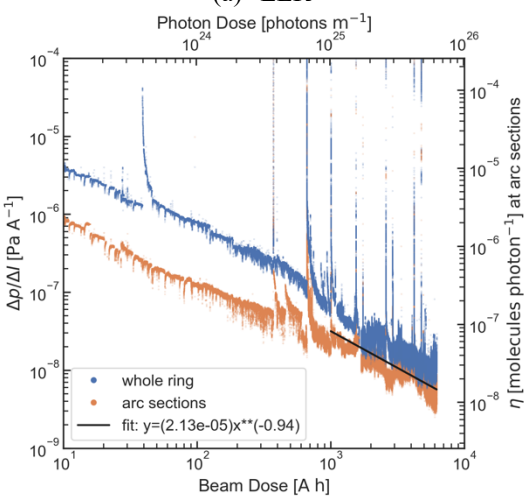

(b) HER

Figure 4: Pressure increase per unit beam current $\Delta p/\Delta I$ and PSD coefficient η at arc sections as a function of beam dose and photon dose in (a) the LER and (b) the HER from February 1st, 2016 to June 22nd, 2022. Result of regression analysis for whole rings from Phase 3 (1112.6 to 7312.1 A h in LER and 1001.9 to 6199.0 A h in HER) with $\Delta p/\Delta I = a \times (\text{beam dose})^b$, where a and b are constants, are also shown.

Residual Gas Species

Figure 5 shows the partial pressure normalized by the beam current in the LER, measured with a residual gas analyzer (RGA) during the 2019 spring run from March 11th to July 1st. It can be seen that the partial pressure of the residual gas decreased as the operating time progressed, indicating that vacuum scrubbing progressed. The RGA measuring this partial pressure is installed near an ion pump in the Tsukuba straight section of the LER, which is upstream of the interaction point.

The main gas species detected during this operation were hydrogen, carbon monoxide, water, methane, carbon dioxide, and oxygen derived from cracking of water, which are typical gas species emitted by PSD. During the shutdown period before the start of this operation, this section was once exposed to the atmosphere for vacuum works and, as a result, the partial pressure of water during this period was relatively high at the beginning of the operation.

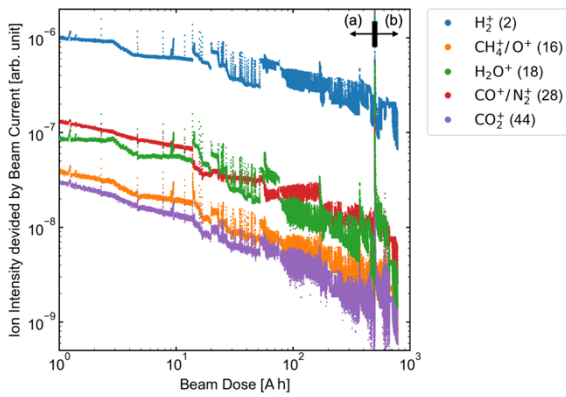

Figure 5: Ion intensity per unit beam current measured by an RGA installed in the Tsukuba straight section of the LER during (a) the spring and (b) the autumn run of 2019. The secondary-electron multiplier of the RGA was used in these measurements. Values in parentheses in the legend refer to the mass-to-charge ratio.

MAJOR PROBLEMS

In this section, we report the major problems that occurred in the SuperKEKB main ring and hindered its operation.

Cooling-Water-System Failure in the Wiggler Magnet Section

The beam in LER was aborted by the temperature interlock of the vacuum system at 17:22:54 on December 5th, 2020. Fig. 6 shows the beam current and the readings of the thermometer (a resistance temperature detector (RTD), attached to the surface of the bellows chambers in the Nikko wiggler section.

The temperatures rose rapidly, beginning at about 17:17, and the beam was then aborted, when the temperature exceeded the interlock threshold of 100 °C. The cause of this sudden rise in temperature was a failure of the water pumps and inverters in the facilities system, one of the

ISBN: 978-3-95450-236-3 ISSN: 2673-7027 doi:10.18429/JACoW-eeFACT2022-THXAS0102

infrastructures of SuperKEKB, and the water flow for the vacuum system was completely stopped in this section. A mask for SR is placed at downstream of each beam pipe, and the temperature on the SR mask rose due to a stoppage of the water flow. The temperature then rose rapidly at the flange on one side only, and we speculate that the difference in thermal expansion between the flanges caused a plastic deformation of the gaskets at that time. Later, at around 17:42, a backup pump in the cooling-water system was started, causing the temperature to drop rapidly.

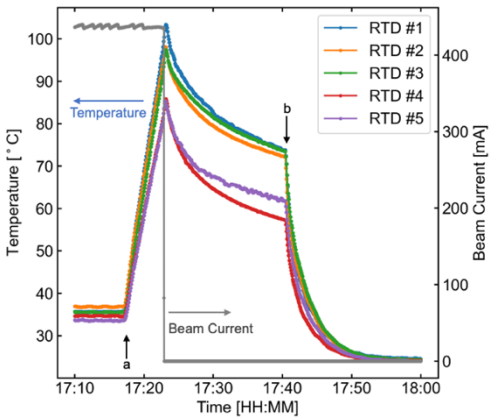

Figure 6: Temperatures of the bellows chambers in Nikko wiggler section and the beam current in the LER. The cooling water system stopped at Point a and resumed at Point b.

A behavior of the pressure after this failure is shown in Fig. 7. When the LER beam decreased or was aborted, the pressure in some CCGs in this section increased accordingly. This suggests that the beam pipes underwent thermal expansion when the beam was stored, and the gasket at the flanges was pinched. Consequently, the leak rate decreased. The beam pipes shrank when the beam was aborted, and the leak rate increased.

A leakage test was then conducted in this section, and leaks were found in a nine of the flanges. These leaks were stopped in three flanges by spraying a liquid sealant (VACSEAL, PASCAL Co. Ltd.) and by tightening the bolts at the others.

It had not been assumed that the flow of water in a section would stop completely due to a failure of the infrastructure, and no interlock system for this purpose had been constructed. Consequently, after this problem, we reconsidered the interlock system and we took appropriate countermeasures, such as issuing beam-abort requests when the water flowrate in the pumping system of the infrastructure dropped.

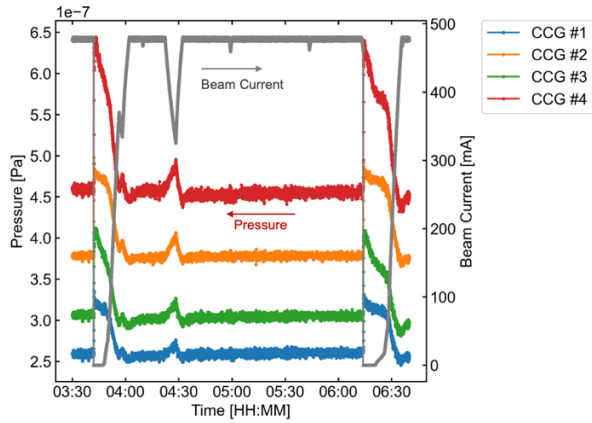

Figure 7: Pressure measured with CCG in Nikko wiggler section and beam current in LER when there are leaks.

Collimator Damage Due to Kicker Accidentally Firing

Because of the narrow physical aperture, there have been many instances in which the beam hit the jaws of the collimators, damaging them [14]. Huge beam-loss events that damage the vertical collimators are called sudden beam losses because it was observed that the beam trajectory suddenly shifted in two to three turns (20–30 μs) before being aborted [16,17]. The cause of this beam loss is still unknown.

There were also damage events for known reasons, such as damage to horizontal collimators caused by accidental firings of injection kickers in the LER. Each set of injection kickers for the main ring consists of three magnets, and two of these sets are installed with a septum magnet in between. Since a thyratron power supply drives the kicker magnet with a one-to-one correspondence, if one of the thyratrons fires and kicks the stored beam horizontally, there is nothing to kick back, so the beam hits the horizontal collimator, which has the narrow horizontal aperture downstream of the injection kickers. The beam current then had to be reduced during the operation until the frequency of accidental firings decreased.

The horizontal position of the center of gravity for each bunch, as measured with a bunch oscillation recorder [18] at the time of an accidental firing is shown in Fig. 8. The harmonic number of the main ring is 5120. Currently, the SuperKEKB main ring operates with two trains and two gaps, referred to as abort gaps, to avoid kicking the bunch on the rising of a kicker for the beam aborts. When a kicker fired accidentally, a part of the first train received a substantial kicking and was lost, as shown in Fig. 8(b). The stored beam was aborted on the next turn.

Content from this work may be used under the terms of the CC-BY-4.0 licence (© 2022). Any distribution of this work must maintain attribution to the author(s), title of the work, publisher, and DOI

ISBN: 978-3-95450-236-3 ISSN: 2673-7027 doi:10.18429/JACoW-eeFACT2022-THXAS0102

Content from this work may be used under the terms of the CC-BY-4.0 licence (© 2022). Any distribution of this work must maintain attribution to the author(s), title of the work, publisher, and DOI

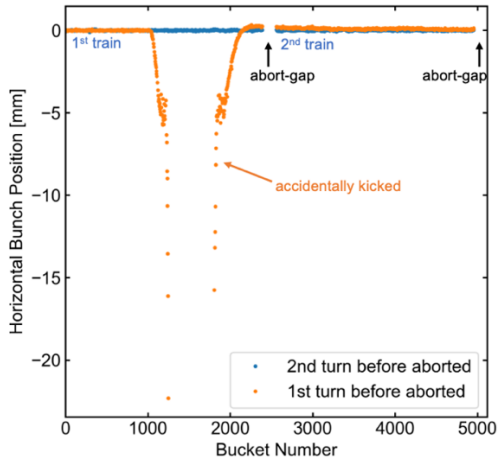

Figure 8: Horizontal position of the center of gravity for each bunch measured with a bunch oscillation recorder and the bucket number when an accidental firing of an injection kicker occurred.

At this time, a pressure burst was observed by the CCG installed near the horizontal collimator named D06H3, as shown in Fig. 9, indicating that the beam hit the jaw.

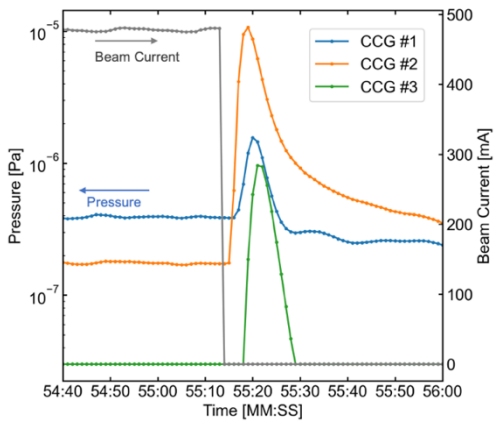

Figure 9: Pressure near D06H3 collimator and beam current in LER when an accidental-firing occurred. CCG #2 is a vacuum gauge closest to the collimator. The distance between the vacuum gauge and the tip of the jaw is approximately 1.2 m for CCG #1, 6.3 m for CCG #2, and 9.3 m for CCG #3.

Figure 10 shows the tip of a jaw located at the inner side of the ring taken from the D06H3 collimator during a shutdown period. The tip was made of tungsten, and it had a large crack and was damaged. Because the probability of a thyratron accidentally firing cannot be reduced to zero, we are developing a robust jaw made of carbon-fiber-reinforced carbon (CFC) as a countermeasure against such an event [16].

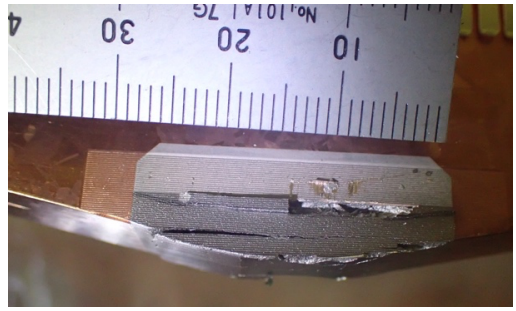

Figure 10: Photograph of a broken tungsten jaw from D06H3.

MINOR INCIDENTS

In this section, we report minor incidents that did not directly affect the operation of the accelerator.

Water Leak in a Collimator's Jaw

During the shutdown period before the start of Phase 3 in 2019, some collimators were newly installed to the main ring. After the installation of the horizontal collimator named D02H1 in the LER, when we ran the cooling water system after rough pumping with a turbomolecular pump (TMP), the high voltage of the CCGs near the collimator was turned off due to an interlock because the pressure increased to the order of 10^{-2} Pa and the number of rotations in the TMP also dropped.

The jaw of the collimator incorporates a cooling-water channel to remove the heat load caused by SR. Because the CCGs near the collimator were turned off when the water flowed, we suspected that there was a leak from the channel to the vacuum chamber. When the water in the channel was removed, the pressure decreased from 10^{-2} to 10^{-3} Pa. However, when a leak test was conducted on the cooling channel, no leak was detectable by simply spraying helium into it, and the leak was detected only after pressurizing the helium to 0.3 MPa. The leak rate was about 1×10^{-5} Pa m^3 s^{-1}.

After removing the jaw, a leak test was performed with a sniffer probe and leak-detection liquid. The leak rate in the channel, as determined by the sniffing scheme for pressurized helium, was $\sim 5.6 \times 10^{-4}$ Pa m^3 s^{-1}, and the leakage point was at a joint between copper and stainless-steel, as shown in Fig. 11.

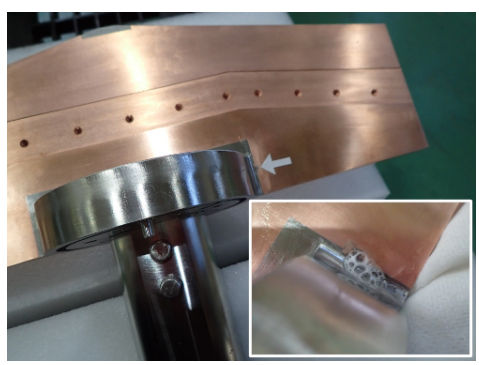

Figure 11: Leakage point of the jaw, as detected by a leak test using a foaming liquid.

ISBN: 978-3-95450-236-3 ISSN: 2673-7027 doi:10.18429/JACoW-eeFACT2022-THXAS0102

Inside this part, a stainless-steel block for the flange and a stainless-steel pipe are welded by tungsten–inert-gas (TIG) welding. In the production of the jaws, the flange and water-channel parts are sandwiched between copper blocks, and a heavy metal such as tungsten or tantalum is placed on the tip and the parts joined by hot isostatic pressing. After joining, these parts were processed into the final shape, and a part of the bead formed by the TIG welding was scraped during this processing, causing the leak.

Before the delivery of the jaws, the cooling water channel was pressurized to ~1.2 MPa with nitrogen, and a leak test was conducted by monitoring the pressure drop with a pressure gauge for at least 10 minutes; however, the item passed the test. In the jaws currently being manufactured, the structure has been improved to prevent scraping of the welding bead. In addition to a rough leak test by monitoring the pressure drop, a precise leak test of the channel with pressurized helium and a leak detector is conducted.

The remanufactured jaw was reinstalled in D02H1 for the 2019 spring operation, but it was difficult to decrease the pressure around this collimator. We consider that this is because the water that leaked at the time of the leak remained in the chamber. Therefore, the entire collimator chamber and beam pipes near it were baked in the tunnel during the 2019 summer shutdown, as shown in Fig. 12.

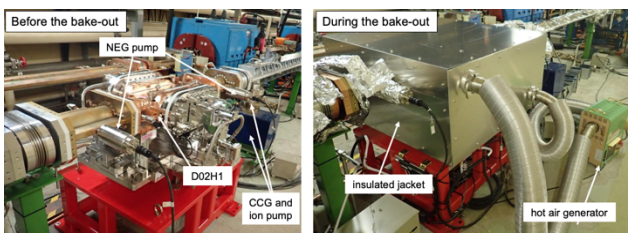

Figure 12: Photographs of the D02H1 collimator before and during baking.

Figure 13 shows the values of $\Delta p/\Delta I$ for a CCG near the D02H1 collimator during the 2019 spring and autumn runs.

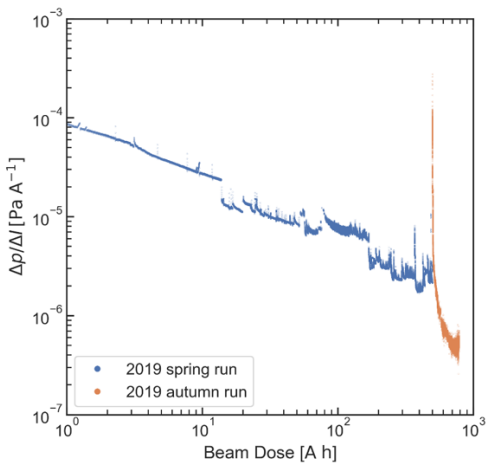

Figure 13: Pressure increase per unit beam current $\Delta p/\Delta I$ as a function of the beam dose for 2019 spring and autumn runs.

After baking, the $\Delta p/\Delta I$ value for the latter decreased rapidly by a factor of approximately six with further beam dose, indicating that baking in situ is an effective method for pumping water out of the chamber.

Abnormal Pressure Increase

Pressure increases during the beam operation have been observed in some vacuum-related components. Here, we report the case of a chamber for a luminosity monitor as an example. The luminosity monitor, named the Zero Degree Luminosity Monitor (ZDLM [19]), is installed downstream of the interaction point in the LER. As shown in Fig. 14, the beam pipe for the ZDLM has a structure in which the location where the sensor is installed protrudes toward the beam.

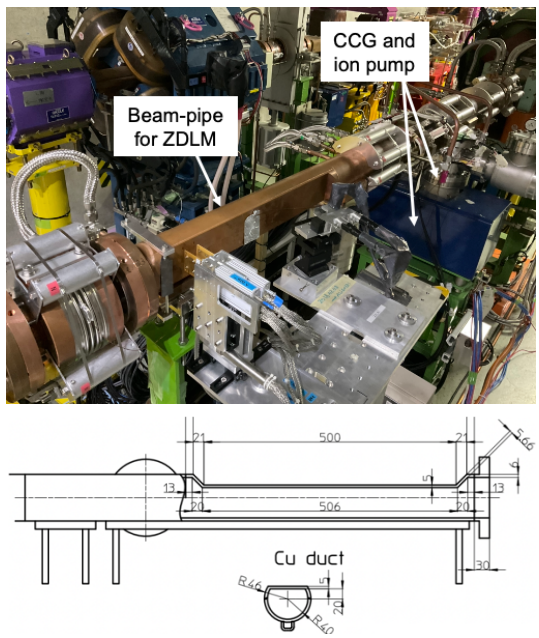

Figure 14: Photograph and drawing of the beam pipe for ZDLM.

The loss factor k_z [V C^{-1}] for a vacuum component characterizes the energy loss ΔE [J] of a bunch due to beam-impedance interaction in the longitudinal direction as the bunch passes through the component, and the energy loss can be calculated as follows:

$$\Delta E = k_z q^2, \tag{4}$$

where q is the bunch charge. The loss factor k_z in terms of the wake potential in the longitudinal direction $W_z(s)$ can then be written as:

$$k_z = \int_{-\infty}^{\infty} W_z(s)\lambda(s)\,ds \tag{5}$$

$$\lambda(s) = \frac{1}{\sqrt{2\pi}\sigma_z}\exp\left(-\frac{s^2}{2\sigma_z^2}\right), \tag{6}$$

where $\lambda(s)$ is the longitudinal charge density in the bunch. Therefore, the beam power loss due to the loss factor of a vacuum component can written as

$$P = \frac{\Delta E}{T_b} = k_z I^2 T_b\,, \tag{4}$$

Content from this work may be used under the terms of the CC-BY-4.0 licence (© 2022). Any distribution of this work must maintain attribution to the author(s), title of the work, publisher, and DOI

ISBN: 978-3-95450-236-3 ISSN: 2673-7027 doi:10.18429/JACoW-eeFACT2022-THXAS0102

Content from this work may be used under the terms of the CC-BY-4.0 licence (© 2022). Any distribution of this work must maintain attribution to the author(s), title of the work, publisher, and DOI

where P is the beam power loss [W], I is the beam current [A], T_b is the bunch [s], because $q = IT_b$. The lost beam power is finally wasted through heating of the surrounding vacuum components.

The wake potential of the beam-pipe for the ZDLM and a SuperKEKB-type horizontal collimator [14], calculated by *GdfidL* for a bunch length (σ_z) of 6 mm, is shown in Fig. 15. The horizontal collimator is one of the main sources of impedance in the ring. However, the loss factor in this beam pipe is ~0.18 V pC^{-1}, which is ~4.5 times larger than the loss factor of ~0.04 V pC^{-1} in the horizontal collimators because the wake potential in this beam-pipe is resistive, as shown in Fig. 15. The beam power loss in the beam-pipe and the collimator are then estimated to be ~1.08 kW and ~0.24 kW, respectively, for a beam current of 1.0 A and three-bunch spacing (6 ns).

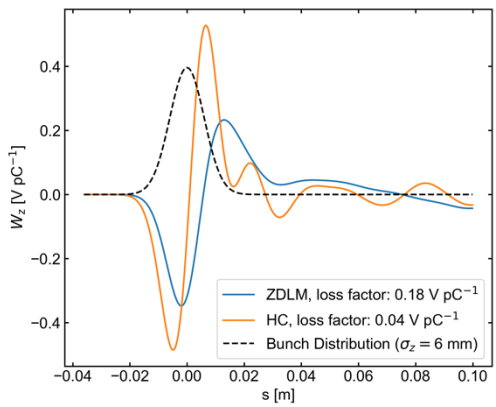

Figure 15. Longitudinal wake potential for the beam pipe for the ZDLM and the SuperKEKB-type horizontal collimator. Also plotted are the bunch distribution of σ_z = 6.0 mm. In the legend, ZDLM and HC refer to the beam-pipe for the ZDLM and the SuperKEKB-type horizontal collimator.

Pressure increases have been observed near this beam pipe, as shown in Fig. 16.

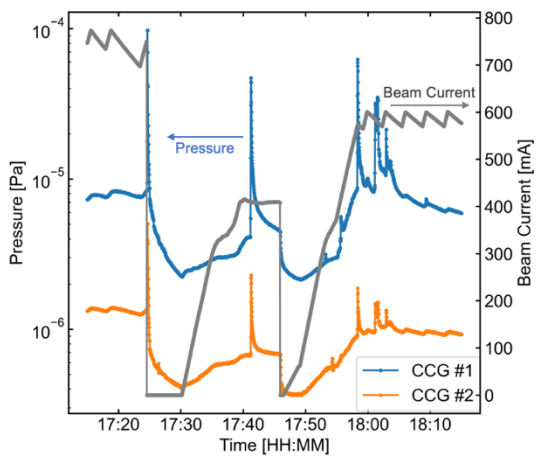

Figure 16: Pressure near the beam pipe for the ZDLM and the beam current in the LER during Phase 2 operation. The distance between the vacuum gauge and the beam pipe is approximately 1m for CCG #1 and 6 m for CCG #2.

When the LER beam current is ~800 mA, the surface temperature of this beam pipe is ~40 °C. At the same beam current, the temperature of the beam pipes in the arc sections is ~25 °C. Therefore, it is possible that the beam power loss due to the beam-impedance interaction in this beam pipe results in the pipe warming itself and nearby components, and the electromagnetic field excited in the structure might cause discharges in the slit structure of the pumping port. The observed frequency of pressure increases has been decreasing, suggesting that there is an aging effect. At present, these pressure increases do not hinder beam operations, but it may become a problem if the beam current is increased in the future.

CONCLUSION

Since the start of their operating period, newly installed components of the vacuum system of SuperKEKB have generally worked as expected. We have identified and reported some problems that occurred up to the present. Some topics that are not discussed here, such as beam-current-dependent pressure increases, beam lifetime determination by vacuum pressure, and electron-cloud instability will be addressed later [21].

ACKNOWLEDGEMENTS

We thank all the staff of the SuperKEKB accelerator and Belle II detector for their cooperation.

REFERENCES

[1] Y. Ohnishi *et al.*, "Accelerator design at SuperKEKB", *Prog. Theor. Exp. Phys.*, vol. 2013, n.3, p. 03A011, 2013. doi:10.1093/ptep/pts083

[2] Y. Suetsugu *et al.*, "Results and problems in the construction phase of SuperKEKB", *J. Vac. Sci. Technol. A*, vol. 34, p. 021605, 2016. doi:10.1116/1.4942455

[3] Y. Suetsugu *et al.*, "First Commissioning of the SuperKEKB Vacuum System", *Phys. Rev. Accel. Beams,* vol. 19, p. 121001, 2016. doi:10.1103/PhysRevAccelBeams.19.121001

[4] Y. Suetsugu *et al.*, "Achievements and problems in the first commissioning of SuperKEKB vacuum system", *J. Vac. Sci. Technol. A,* vol. 35, p. 03E103, 2017. doi:10.1116/1.4977764

[5] Y. Suetsugu *et al.*, "SuperKEKB main ring vacuum system status until the end of Phase-2 commissioning", *J. Vac. Sci. Technol. A* , vol. 37, p. 021602, 2019. doi:10.1116/1.5083928

[6] K. Shibata *et al.*, "Commissioning of vacuum system for SuperKEKB positron damping ring", *J. Vac. Sci. Technol. A*, vol. 37, p. 41601, 2019. doi:10.1116/1.5092956

[7] Y. Funakoshi et al., "The SuperKEKB has Broken the World Record of the Luminosity", *Proc. IPAC'22*, Bangkok, Thailand, Jun. 2022, pp. 1-5. doi:10.18429/JACoW-IPAC2022-MOPLXGD1

[8] "Operation status and plan on SuperKEKB", https://www-linac.kek.jp/skekb/status/web/status_plan.md.html.

ISBN: 978-3-95450-236-3 ISSN: 2673-7027 doi:10.18429/JACoW-eeFACT2022-THXAS0102

[9] K. Shibata *et al.*, "Commissioning Status of SuperKEKB Vacuum System", *Proc. eeFACT2018*, Hong Kong, China, 2018, WEOAB01, pp.226–233.

[10] Y. Suetsugu *et al.*, "Beam scrubbing of beam pipes during the first commissioning of SuperKEKB vacuum system", *Appl. Surf. Sci.*, vol. 432, Part B, p. 347, 2018. doi:10.1016/j.apsusc.2017.06.162

[11] Y. Suetsugu *et al.*, "Mitigating the electron cloud effect in the SuperKEKB positron ring", *Phys. Rev. Accel. Beams*, vol. 22, p. 023201, 2019. doi:10.1103/PhysRevAccelBeams.22.023201

[12] Y. Suetsugu *et al.*, "Study to Mitigate Electron Cloud Effect in SuperKEKB", *Proc. eeFACT2018*, Hong Kong, China, 2018, TUYAA04, pp. 95–102.

[13] Y. Suetsugu *et al.*, "Development of bellows and gate valves with a comb-type rf shield for high-current accelerators: Four-year beam test at KEK B-Factory", *Rev. Sci. Instrum.*, vol. 78, p. 043302, 2007. doi:10.1063/1.2723747

[14] T. Ishibashi *et al.*, "Movable collimator system for SuperKEKB", *Phys. Rev. Accel. Beams*, vol. 23, p. 53501, 2020. doi:10.1103/PhysRevAccelBeams.23.053501

[15] O. Gröbner *et al.*, "Studies of photon induced gas desorption using synchrotron radiation", *Vacuum*, vol. 33, p. 397, 1983. doi:10.1016/0042-207X(83)90659-0

[16] S. Terui *et al.*, "Development of Low-Z Collimator for SuperKEKB", *Proc. of PASJ2020*, 2020, FROT07, pp. 197–201. (in Japanese)

[17] S. Terui *et al.*, "Report on Collimator Damaged Event in SuperKEKB", *Proc. IPAC'21*, Campinas, Brazil, 2021, May 2021, pp. 3541-3544. doi:10.18429/JACoW-IPAC2021-WEPAB359WEPAB359

[18] M. Tobiyama *et al.*, "Development of Bunch Current and Oscillation Recorder for SuperKEKB Accelerator", *Proc. IBIC'12*, Tsukuba, Japan, 2012, MOPA36, pp. 138–142.

[19] P. Bambade *et al.*, "Fast Luminosity Monitoring for the SuperKEKB Collider", *Proc. eeFACT2018*, Hong Kong, China, 2018, TUPBB06, pp. 173–178.

[20] GdfidL, http://www.gdfidl.de/

[21] Y. Suetsugu *et al.*, "SuperKEKB Vacuum System in these Six Years Operation", in *Proc. IVC-22*, Sapporo, Japan, Sep. 11-16, 2022, to be published.

Content from this work may be used under the terms of the CC-BY-4.0 licence (© 2022). Any distribution of this work must maintain attribution to the author(s), title of the work, publisher, and DOI